Thin Solid Films 518 (2010) 1953–1957

Contents lists available at ScienceDirect

Thin Solid Films

journal homepage: www.elsevier.com/locate/tsf

Relation between the plasma characteristics and physical properties of functional zinc oxide thin film prepared by radio frequency magnetron sputtering process

Che-Wei Hsu [a], Tsung-Chieh Cheng [b], Wen-Hsien Huang [c], Jong-Shinn Wu [a,*], Cheng-Chih Cheng [a], Kai-Wen Cheng [a], Shih-Chiang Huang [c]

[a] *Department of Mechanical Engineering, National Chiao Tung University, 1001 Ta-Hsueh Road, Hsinchu 30050, Taiwan*
[b] *Department of Mechanical Engineering, National Kaohsiung University of Applied Science, 415 Chien Kung Road, Kaohsiung 807, Taiwan*
[c] *National Nano Device Laboratories, No. 26, Prosperity Road I, Science-based Industrial Park, Hsinchu 30078, Taiwan*

ARTICLE INFO

Article history:
Received 13 November 2008
Received in revised form 14 July 2009
Accepted 27 July 2009
Available online 4 August 2009

Keywords:
Zinc Oxide
Ion bombardment
Optical properties
Radio-frequency sputtering
UV protection coatings

ABSTRACT

The ZnO thin film was deposited on a glass substrate by a RF reactive magnetron sputtering method. Results showed that plasma density, electron temperature, deposition rate and estimated ion bombardment energy increase with increasing applied RF power. Three distinct power regimes were observed, which are strongly correlated with plasma properties. In the low-power regime, the largest grain size was observed due to slow deposition rate. In the medium-power regime, the smallest grain size was found, which is attributed to insufficient time for the adatoms to migrate on substrate surface. In the high-power regime, relatively larger grain size was found due to very large ion bombardment energy which enhances the thermal migration of adatoms. Regardless of pure ZnO thin film or ZnO on glass, high transmittance (>80%) in the visible region can be generally observed. However, the film thickness plays a more important role for controlling optical properties, especially in the UV region, than the applied RF power. In general, with properly coated ZnO thin film, we can obtain a glass substrate which is highly transparent in the visible region, is of good anti-UV characteristics, and is highly hydrophobic, which is highly suitable for applications in the glass industry.

© 2009 Elsevier B.V. All rights reserved.

1. Introduction

In recent years, Zinc Oxide (ZnO) is one of the promising candidate materials which has been extensively investigated for various applications in many fields, such as optoelectronics (e.g., light emitting diode [1–3], transparent conductive oxide [4,5] and solar cell or photovoltaic [6]), piezoelectric [7], sensors [8], and energy and environment (e.g., heat-reflecting coating [9], and architectural windows [10–12]), to name a few. Wide applications of ZnO thin film arise from several unique material properties, including a hexagonal wurtzite structure and wide direct band gap of 3.37 eV at room temperature (RT). In addition, ZnO film also possesses highly conductive, chemically and thermally stable properties, and has high piezoelectric coupling coefficient. Therefore, ZnO is considered as one of the most interesting semiconductors of II–VI compounds with a wide range of scientific and technological importance.

By the way, overdosed ultraviolet (UV) irradiation has become a serious problem due to ozone depletion globally. How to prevent the UV light from direct contact with human while allowing most of the visible light to fill in the living space is a critical issue in modern glass industry [13]. In addition, a highly hydrophobic glass surface is also strongly necessary, which can greatly reduce the cost of maintenance. Thus, development of coating on glass surface, which is high transparent in the visible, has anti-ultraviolet (anti-UV) characteristics, and has self-clean capability, is very important for the glass industry. Till now, many studies have focused on the measurements of transmittance in the visible and enhanced hydrophobic characteristics of ZnO thin film, while almost none has paid attention to simultaneous characterization of high transmittance in the visible, high absorbance in the UV, and self-clean capability, which is otherwise very important for applications in glass industry such as architectural windows or automotive windshields industry and so on.

ZnO films have been grown by various deposition methods, such as sputtering [14–24], chemical bath deposition [25], spray pyrolysis [26], pulsed laser deposition [27,28], and metal organic chemical vapor deposition [29]. Sputtering method represents one of the simplest and most effective methods. In the past, many researchers have studied in correlating the radio frequency (RF) power with the several physical properties of deposited film [e.g., 17–20 and references cited therein]. But, very few researchers have simultaneously correlated the detailed plasma parameters, in addition to RF power, with film properties [e.g., 30,31]. However, it is well known that the film quality is directly controlled by the plasma conditions. Understanding of the relationship between plasma conditions and thin-film properties should greatly help to produce high-quality ZnO thin film. Thus, it is very crucial to understand the correlation between these characteristics in detail. In the

* Corresponding author. Tel.: +886 3 573 1693; fax: +886 3 572 0634.
E-mail address: chongsin@faculty.nctu.edu.tw (J.-S. Wu).

0040-6090/$ – see front matter © 2009 Elsevier B.V. All rights reserved.
doi:10.1016/j.tsf.2009.07.181

present study, we focus on investigating and demonstrating the importance of deposition rate and ion bombardment energy to growth process of ZnO thin film. In addition, relation between deposition rates, plasma conditions and general physical properties (structural, optical, and hydrophobic) of the ZnO thin films is also addressed in this paper.

2. Experimental setup

Fig. 1 illustrates the schematic diagram of the RF reactive magnetron sputtering system along with a Langmuir probe system which is used to measure the plasma properties inside the chamber. In the current study, a 4 inch diameter Zn target (99.999%) is used. Argon (99.999%) and oxygen (99.999%) are used as the working (discharge) and reactive gas, respectively. These two gases are mixed prior to entering the sputtering chamber with a predetermined ratio in mass flow rate. Distance between the target and substrate is kept as 8 cm unless otherwise specified. The normal procedures of operating the sputtering chamber include: 1) Evacuate the chamber to a base pressure below 1.0×10^{-4} Pa (8.0×10^{-7} Torr) through roughing and cryo pumps; 2) Send the mixed argon–oxygen gas through the chamber for 10 min while maintaining the chamber pressure at 2 Pa (15 mTorr); 3) Pre-sputter the chamber for 20 min with RF power of 100 W, which is used to remove any possible contamination or oxides from the Zn target surface.

In the present study, the ZnO thin film was deposited on micro-slide glass substrate at RT by a RF reactive magnetron sputtering method. ZnO thin films were grown using the mixture with a fixed volume ratio of $O_2/(Ar+O_2)$ as 0.5 at a constant working pressure of 2 Pa (15 mTorr). Two major test conditions for preparing ZnO thin film include: 1) Deposition time ranges from 5 to 60 min with a constant RF power of 100 W; 2) RF power ranges from 50 to 400 W with a constant film thickness of 60 nm.

An automatic motor-driven Langmuir probe inserted into the gas discharge through the sidewall of sputtering chamber is used to measure plasma parameters which include floating potential (V_f), plasma potential (V_s), electron temperature (T_e), electron number density (n_e), and ion number density (n_i) [30–34]. This Langmuir probe system is a cylindrical type made by Hiden Analytical Inc (Model: Hiden ESPion). The probe tip was placed at the plasma bulk region with 2 cm from the substrate along the center line. The bias voltage (V) applied to the Langmuir probe ranges from −50 V to 70 V in the present measurements. Film thickness was measured by a surface profilometer (Model 3030, Sloan Dektak Inc.). Crystal structure and orientation of the films were determined by the X-ray diffraction (XRD) technique using CuKα radiation (λ = 1.5418 Å) (Model: PANalytical X'Pert Pro (MRD), Philips X'Pert Inc.), which was operated at 45 kV and 40 mA for Gonio and GIXRD scan. Optical transmittance of the ZnO films was measured using a UV–VIS spectrophotometer (Shimadzu Inc., Model UV-2501PC).

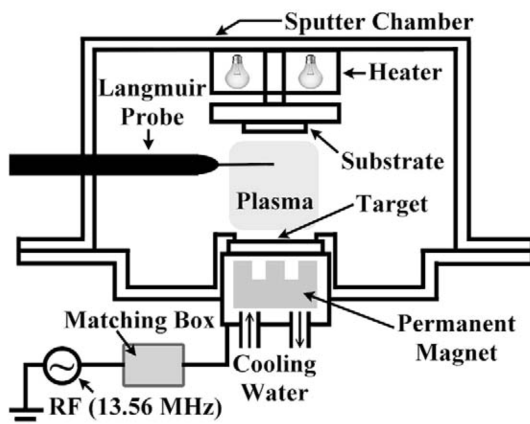

Fig. 1. Schematic diagram of the RF reactive magnetron sputtering chamber with instrumentation.

Contact angle was observed by a contact angle system with a universal surface tester (KRŰSS Inc., model GH-100).

3. Results and discussion

3.1. Plasma characteristics

Fig. 2a and b illustrates several measured plasma parameters of sputtering process as a function of RF power. Both the electron number density (n_e) and positive ion number density (n_i) increase with increasing RF power. This is because the electrons are accelerated under increasingly high oscillating electric field, obtain increasingly high energy (higher T_e), and result in increasingly high ionization probability with increasing RF power, as shown also in Fig. 2a. This will increase the ion flux (Fig. 2b) and thus the sputtering yield, which results in the higher deposition rate at higher RF powers, as shown in Fig. 3. It is also believed that difference between the number densities of electrons and positive ions represents approximately the total number density of negative charge species (O^-, O_2^-, etc.) in this electronegative (Ar/O_2) plasma. In addition, both the ion bombardment energies (V_s–V_f) [30,31], which are estimated by calculating the difference between plasma potential and floating potential, and positive ion flux are shown in Fig. 2b as a function of RF power. Therefore, both the plasma number density in the bulk and ion bombardment energy onto the Zn target increase with increasing RF power. Thus, most ZnO particles can be formed by reacting with atomic oxygen in the discharge [34,35] as the RF power is higher. The ion bombardment energy generally increases with increasing RF power, except the case when the RF power is 50 W. Note that the increase of electron temperature from RF power of 50 W to 200 W becomes small probably due to the slightly decrease of (V_s–V_f). In general, the measurements shown in Fig. 2 demonstrate that the plasma becomes stronger as the RF power increases.

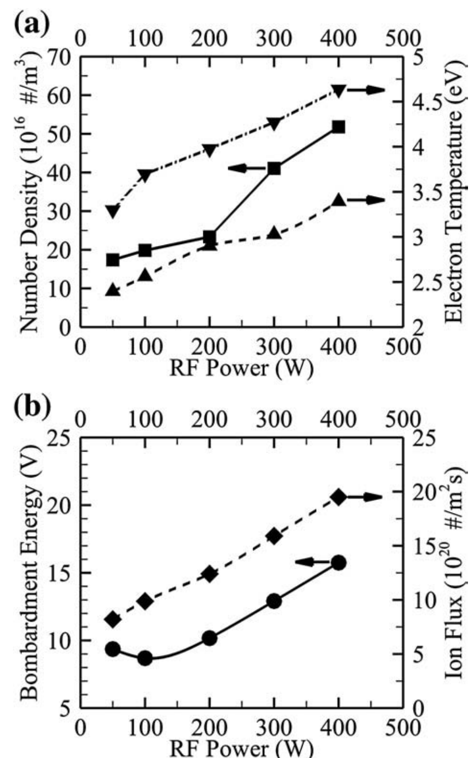

Fig. 2. (a) Electron number density (▲), ion number density (▼), and electron temperature (■); (b) bombardment energy (●) and ion flux (♦) as a function of applied RF power in an Ar/O_2 plasma used for ZnO thin film deposition.

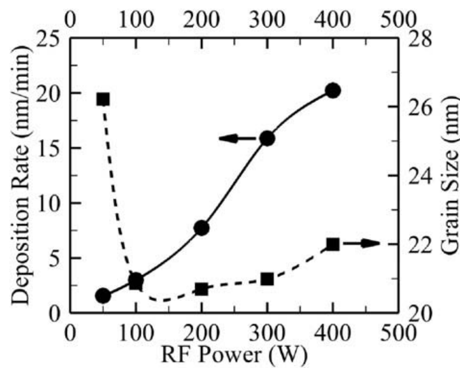

Fig. 3. The deposition rate (●) and the calculated grain size (■) as a function of applied RF power in an Ar/O_2 plasma used for ZnO thin film deposition.

Fig. 3 shows the deposition rate and grain size as a function of RF power. In general, the deposition rate increases monotonically with increasing RF power, which is strongly correlated with incident ion flux towards the substrate as shown in Fig. 2b. Based on the Scherrer equation [36], the grain size is calculated by the observed XRD patterns. Grain size decreases rapidly from 26.22 nm at 50 W down to 20.7 nm at 100 and 200 W, and then increases gradually up to 22 nm at 400 W. In contrast with the almost monotonically increasing deposition rate with increasing RF power, the estimated ion bombardment energy and grain size first decrease and then increase with increasing RF power. We attribute the observed unusual trend of grain size to the three distinct power regimes which are detailed in the following.

In the low-power regime (50 W), the largest grain size appears corresponding to the slowest deposition rate because of the lowest ion flux, as shown in Fig. 2b. Thus, crystal growth is mostly deposition rate controlled, in which the ion bombardment energy and plasma density are both small. In the medium-power regime (100–200 W), higher ion flux (and higher plasma density) with still low ion bombardment energy (8.7–10.2 eV) and thus higher ZnO particle flux towards the substrate causes adverse effect on crystal growth since there is insufficient time for adatoms migration on the substrate. Hence, the lowest grain size is observed in this regime. In the high-power regime (300–400 W), very high ZnO particle flux migrates towards the substrate, but with very high ion bombardment energy (12.9–15.8 eV), which can help heat up the substrate and enhance thermal diffusion of the adatoms on the substrate, and thus favors the crystal growth of the ZnO thin film [20]. Thus, the grain size increases with increasing RF power in this regime and is mainly ion bombardment energy controlled.

3.2. Structural properties

Based on Fig. 4a and b, all of these ZnO thin films are in polycrystalline phase with a hexagonal structure (the powder-diffraction file No. 79-0208) and the major orientation is (0002). Fig. 4a exhibits the thickness effect on the ZnO thin films. Results clearly show that the ZnO thin films grown less than 10 min (smaller than 50 nm in thickness) are almost in amorphous phase. It has been shown that the initial ZnO crystallization phase strongly depends on the morphology of substrate surface, which showed that amorphous ZnO forms on an amorphous substrate, polycrystalline ZnO forms on a polycrystalline substrate, and so on [37]. As the ZnO thin film grows over 20 min (large than 60 nm in thickness), crystalline structure of orientation (0002) begins to appear and become dominant in the film structure with further increasing of deposition time.

In addition, Fig. 4b presents the power effect on grown ZnO thin films with approximately 60 nm in thickness. Results show that ZnO thin films with enough film thickness are dominated by the (0002) orientation no matter what the RF power is, although the peak intensity increases obviously with increasing RF power. At the same time, the relative peak intensities of orientation $(10\bar{1}0)$ and $(10\bar{1}1)$ reduce gradually with increasing RF power. This corresponds to the phenomenon of "evolutionary selection" or "survival of the faster" [19], which was first proposed by van der Drift [38] that he used to explain the preferred orientation of a vapor-deposited PbO layer. As mentioned in the above, it seems reasonable to conclude that increasing RF power promotes the growth of the preferred orientation (0002) and hinders the growth of the other orientation $(10\bar{1}0)$ and $(10\bar{1}1)$. By the way, increasing RF power also increases the substrate temperature during the deposition process due to increasing ion bombardment energy. Thus, the ZnO film quality (the narrower FWHM and the larger grain size) improves with increasing surface mobility because of increasing substrate temperature with RF power more than 200 W [33].

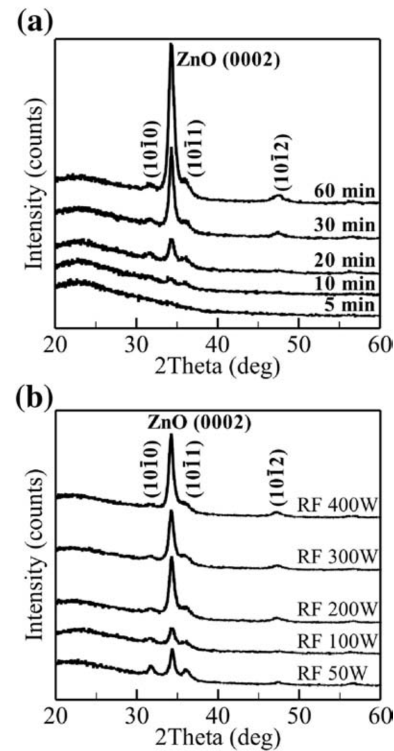

Fig. 4. Effect of (a) deposition thickness (at RF 100 W) and (b) applied RF power (fixed at 60 nm) on XRD pattern of ZnO thin film on glass substrate.

3.3. Optical properties

Fig. 5a and b shows the measured transmittance of ZnO thin film with different film thicknesses and RF powers, respectively. Firstly, from Fig. 5a, it is found that the average transmittance of pure ZnO thin film ($T_{ZnO,ave}$%) in the visible range (400–700 nm) decreases from 98% to 86% with deposition time increases from 5 min to 60 min. Correspondingly, the $T_{ZnO,ave}$% in the UV region (280–400 nm) decreases from 80% to 5% with increasing deposition time. Moreover, the inset of Fig. 5a presents the optical transmittance of ZnO thin film on glass substrate ($T_{ZnO/Glass}$%). Results show that anti-UV characteristics of blank glass are only good below some UV wavelength (~280 nm). By combining ZnO thin film with blank glass, we have demonstrated that still high transmittance (80–91%) in the visible region can be obtained, and better anti-UV characteristics are found with increasing deposition time. For example, less than 10% of optical transmittance can be obtained for the wavelength below 350 nm. This shows that very good anti-UV characteristics with excellent optical transmittance in the visible region can be easily obtained on glass,

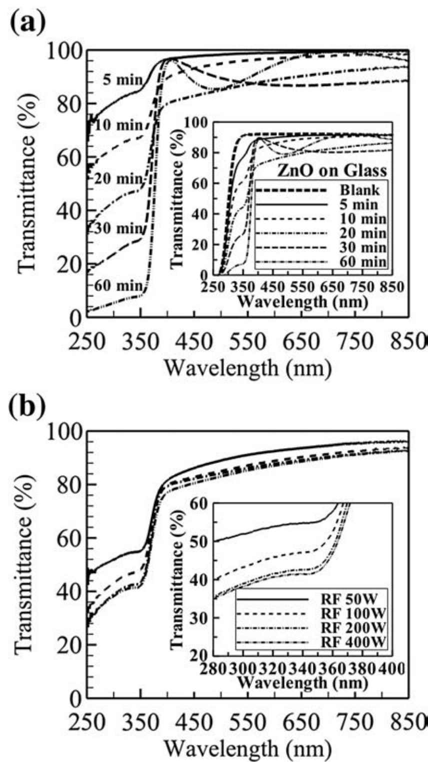

Fig. 5. The transmittance of pure ZnO thin film with (a) effects of thickness and (b) effects of applied RF power. Inset of panels (a) and (b) shows the transmittance of ZnO thin film on glass substrate and the transmittance of pure ZnO thin film in the UV region, respectively.

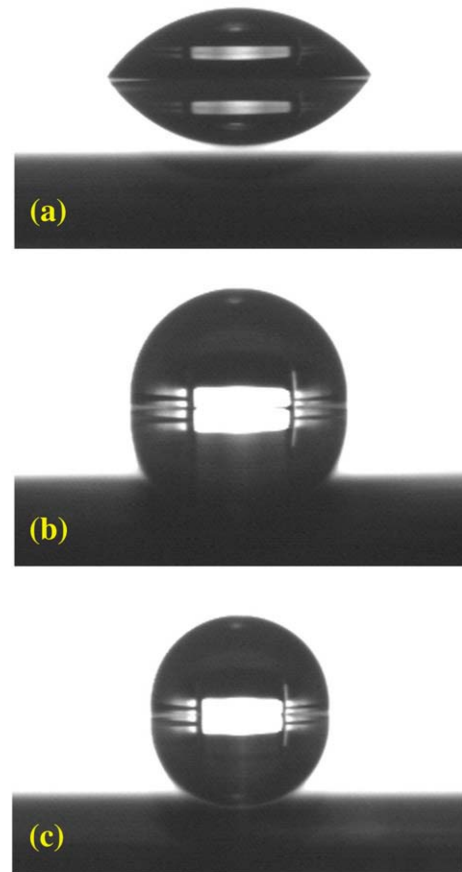

Fig. 6. Hydrophobic characteristics of the glass substrate (a) without ZnO thin film (b) with ZnO thin film at RF 50 W (c) with ZnO thin film at RF 400 W.

should the ZnO thin film thickness is large enough. Secondly, Fig. 5b shows the similar transmittance characteristics (90–86%) in the visible region with the fixed film thickness (60 nm) using different RF powers. In the inset of Fig. 5b, the $T_{ZnO,ave}$% is in the range of 50–41% in the UV spectra, in which the value decreases rapidly with increasing applied RF power from 50 W to 200 W, but it tends to level off at 400 W. In brief summary, effect of varying the RF power with the same ZnO thickness on the optical transmittance from UV to visible is relatively minor [17] as compared to that of varying the film thickness, especially in the UV region.

3.4. Hydrophobic properties

In Fig. 6a, the blank glass substrate exhibits obvious hydrophilic characteristics with contact angle of 52.5°, while in Fig. 6b and c, the glass substrate coated with ZnO thin films shows the increasing hydrophobic property with increasing RF power up to 96° of contact angle. Present results clearly show that the ZnO thin film is able to modify the surface of blank glass substrate from hydrophilic to hydrophobic effectively. This demonstrates that glass substrate coated with ZnO thin film exhibits excellent self-clean characteristics.

4. Conclusion

In the current study, the ZnO thin film was deposited on a glass substrate at RT by a RF reactive magnetron sputtering method. Results show that plasma density, electron temperature, deposition rate and estimated ion bombardment energy increase with increasing RF power. There exists three distinct power regimes, in which the controlling mechanism for the ZnO thin film quality differs, which include: 1) In the low-power regime, the highest grain size is observed due to slow deposition rate; 2) In the medium-power regime, lowest grain size is found; 3) In the high-power regime, both high ion bombardment energy and high plasma density contribute to the higher grain size. The film thickness plays a more prominent role in controlling optical properties, especially in the anti-UV characteristics, than the RF power. In general, with properly coated ZnO thin film, we can obtain a glass substrate which is highly transparent in the visible region, has good anti-UV characteristics, and possesses highly hydrophobic (self-clean capability) characteristics, which is highly suitable for applications in the glass industry.

Acknowledgements

The authors would like to express their sincere thanks to the financial support of National Science Council of Taiwan through NSC 96-2628-E-009-134-MY3 and NSC 96-2628-E-009-136-MY3. Also the instrumentation provided by National Nano Device Laboratory of Taiwan is also highly appreciated. The authors are also thankful to Professor T. C. Wei of the Department of Chemical Engineering, Chung Yuan Christian University, Taiwan for the help in the analysis of plasma theory.

References

[1] Athavan Nadaraah, Robert C. Word, Jan Meiss, Rolf Könekamp, Nano Lett. 8 (2008) 534.
[2] Jae-Kong Lim, Chang-Ku Kang, Kyoung-Kook Kim, Il-Kyu Park, Dae-Kue Hwang, Seong-Ju Park, Adv. Mater. 18 (2006) 2720.
[3] S. Tüzemen, Emre Gür, Opt. Mater. 30 (2007) 292.
[4] John F. Wager, Science 300 (2003) 1245.
[5] Sanghyun Ju, Antonio Facchetti, Yi Xuan, Jun Liu, Fumiaki Ishikawa, Peide Ye, Chongwu Zhou, Tobin J. Marks, David B. Janes, Nat. Nanotechnol. 2 (2007) 378.
[6] A. Shah, P. Torres, R. Tscharner, N. Wyrsch, H. Keppner, Science 285 (1999) 692.
[7] Thomas Thundat, Nat. Nanotechnol. 3 (2008) 133.
[8] Sebastian Polarz, Abhijit Roy, Michael Lehmann, Matthias Driess, frank Einar Kruis, Andreas Hoffmann, Patrick Zimmer, Adv. Funct. Mater. 17 (2007) 1385.

[9] Quan-Bao Ma, Zhi-Zhen Ye, Hai-Ping He, Li-Ping Zhu, Jing-Yun Huang, Yin-Zhu Zhang, Bing-Hui Zhao, Scr. Mater. 58 (2008) 21.
[10] Danny H.W. Li, Joseph C. Lam, Chris C.S. Lau, T.W. Huan, Renew. Energ. 29 (2004) 921.
[11] T. David, S. Goldsmith, R.L. Boxman, Thin Solid Films 447–448 (2004) 61.
[12] E. Ando, M. Miyazaki, Thin Solid Films 516 (2008) 4574.
[13] Marcelo N. Ayala, Ralpb Micbael, Per G. Söderberg, Invest. Ophthalm. Vis. Sci. 41 (2000) 3539.
[14] Sang-Hun Jeong, Bong-Soo Kim, Byung-Teak Lee, Appl. Phys. Lett. 82 (2003) 2625.
[15] Z.Q. Li, D.X. Zangl, J.J. Lin, J. Appl. Phys. 99 (2006) 124906.
[16] K.S. Kim, H.W. Kim, N.H. Kim, J. Mater. Sci. Lett. 22 (2003) 1155.
[17] Kyoung-Kook Kim, Jae-Hoon Song, Hyung-Jin Jung, Won-Kook Choi, Jong-Han Song, Jong-Han Song, J. Appl. Phys. 87 (2000) 3573.
[18] I. Sayago, M. Aleixandre, L. Arés, M.J. Fernández, J.P. Santos, J. Gutiérrez, M.C. Horrillo, Appl. Surf. Sci. 245 (2005) 273.
[19] Kun Ho Kim, Ki Cheol Park, Dae Young Ma, J. Appl. Phys. 81 (1997) 7764.
[20] Yuantao Zhang, Guotong Du, Dali Liu, Xinqiang Wang, Yan Ma, Jinzhong Wang, Jingzhi Yin, Xiaotian Yang, Xiaoke Hou, Shuren Yang, J. Cryst. Growth 243 (2002) 439.
[21] R.J. Hong, X. Jiang, B. Szyszka, V. Sittinger, A. Pflug, Appl. Surf. Sci. 207 (2003) 341.
[22] J.J. Chen, Y. Gao, F. Zeng, D.M. Li, F. Pan, Appl. Surf. Sci. 223 (2004) 318.
[23] Tae-Hyoung Moon, Min-Chang Jeong, Woong Lee, Jae-Min Myoung, Appl. Surf. Sci. 240 (2005) 280.
[24] Z.B. Fang, Z.J. Yan, Y.S. Tan, X.Q. Liu, Y.Y. Wang, Appl. Surf. Sci. 241 (2005) 303.
[25] V.R. Shinde, C.D. Lokhande, R.S. Mane, Sung-Hwan Han, Appl. Surf. Sci. 245 (2005) 407.
[26] Ren-De Sun, Akira Nakajima, Akira Fujishima, Toshiya Watanabe, Kazuhito Hashimoto, J. Phys. Chem. B 105 (2001) 1984.
[27] F.K. Shan, Y.S. Yu, J. Eur. Ceram. Soc. 24 (2004) 1869.
[28] R.D. Vispute, V. Talyansky, Z. Trajanovic, S. Choopun, M. Downes, R.P. Sharma, T. Venkatesan, M.C. Woods, R.T. Lareau, K.A. Jones, A.A. Iliadis, Appl. Phys. Lett. 70 (1997) 2735.
[29] Hyong Woo Kim, Kwang Sik Kim, Chongmu Lee, J. Mater. Sci. Lett. 22 (2003) 1117.
[30] M. Nisha, K.J. Saji, R.S. Ajimsha, N.V. Joshy, M.K. Jayaraj, J. Appl. Phys. 99 (2006) 033304.
[31] T. Nagata, A. Ashida, N. Fujimura, T. Ito, J. Appl. Phys. 95 (2004) 3923.
[32] S.Z. Wu, J. Appl. Phys. 98 (2005) 083301.
[33] Jung W. Lee, Jerome J. Cuomo, Mohamed Bourham, J. Vac. Sci. Technol. A 22 (2004) 260.
[34] R. Cebulla, R. Wendt, K. Ellmer, J. Appl. Phys. 83 (1998) 1087.
[35] S. Im, B.J. Jin, S. Yi, J. Appl. Phys. 87 (2000) 4558.
[36] C. Suryanarayana, M. Grant Notron, X-Ray Diffraction: A Practical Approach, Plenum Press, New York, 1998 p. 212–213.
[37] Y. Yoshino, K. Inoue, M. Takeuchi, K. Ohwada, Vacuum 51 (1998) 601–607.
[38] A. van der Drift, Philips Res. Repts. 22 (1967) 276.